Crystallization of Phenanthrene From Toluene with Carbon Dioxide by the GAS Process

Edwin M. Berends, Odolf S. L. Bruinsma, Jan de Graauw, and Gerda M. van Rosmalen
Lab. for Process Equipment, Delft University of Technology, 2628 CA Delft, The Netherlands

The crystallization of phenanthrene from toluene with carbon dioxide as the antisolvent gas is described. In the GAS process, a pressurized gas is dissolved into a liquid solvent, where it causes a volumetric expansion and lowers the solubility of the solute. Theoretical models are presented for the liquid-phase expansion and the solubility as a function of pressure and temperature. The Nývlt theory for batch crystallization is adapted to predict the pressure profile in the crystallizer needed to maintain a constant supersaturation and growth rate. Generation of seeds is accomplished via a pressure pulse at the saturation pressure. The average particle size of the phenanthrene could be varied from 160 to 540 μm. Creation of seeds doubles the particle size and reduces the coefficient of variation significantly. The residual amount of toluene in the crystals without treatment is approximately 70 ppm. The particles are agglomerates of phenanthrene crystals.

Introduction

The gas antisolvent process (GAS process) is a new technique for crystallization extensively published by Gallagher et al. (1989). The process uses a highly pressurized gas, in the near-critical or supercritical region, as an antisolvent. In the GAS process, a high-pressure gas is dissolved into the liquid-phase solvent, where it causes a volumetric expansion of this liquid solvent and thus lowers the equilibrium solubility. Precipitation of the dissolved compound then occurs. The expanded liquid solvent has higher diffusion coefficients and lower viscosities than normal atmospheric liquids, and a purer product with less solvent inclusions is expected to be formed with this process compared to conventional crystallization processes.

In case of polymers, the addition of an antisolvent first leads to a liquid-liquid phase split into a dispersed polymer-rich phase and a continuous solvent-rich phase (Dixon et al., 1993; Berends, 1994). Addition of more antisolvent will cause extraction of solvent from the polymer-rich phase, and this phase will finally become solid.

In a batch process, the volumetric liquid expansion profile is a function of the temperature, the pressure profile, the type of solvent and antisolvent gas, and the stirring power input. The volumetric liquid expansion profile as a function of the process time determines the rate of supersaturation build-up in the solvent. Particle size and particle-size distribution are expected to be influenced by the volumetric expansion profile.

After the precipitation step, a filtration step is performed at the same pressure and the solvent and antisolvent are easily separated by pressure reduction in a flash vessel. In comparison with conventional salting or drowning out processes, a better control over particle characteristics is expected with average particle size, particle-size distribution, shape and internal structure and residual amount of solvent in the particles.

The aim of the research work presented in this article is to develop the GAS equipment for the crystallization of phenanthrene from toluene with carbon dioxide as the antisolvent gas at 25°C, and to develop theoretical models which should lead to a better understanding and control of the relevant process parameters.

Theory

The supersaturation of the solute in the GAS process is created by dissolving a pressurized gas as an antisolvent into the liquid-phase solvent. The most important process parameters are the equilibrium mole fractions of solvent and antisolvent in the solution, the volumetric expansion of the liquid phase, and the partial molar volumes of the components in the liquid phase that can be calculated with the Peng and

---

Correspondence concerning this article should be addressed to E. M. Berends.

Robinson equation of state (1976). These parameters are calculated as if we are dealing with a binary system: a solvent and an antisolvent. It is assumed that the solute does not have a large influence on these parameters. With these process parameters the equilibrium solubility of the solute is estimated.

The Nývlt theory (Nývlt, 1991) that predicts the temperature curve or evaporation curve needed to maintain a constant supersaturation and growth rate in a batch crystallizer is adapted to predict the pressure profile in the batch GAS crystallizer. Generation of seeds at the saturation pressure can be accomplished via a special technique: a pressure pulse at the saturation pressure.

Expansion of the liquid phase

From the Peng and Robinson equation of state, the equilibrium mole fractions of the solvent and antisolvent and the molar volume of the liquid phase are a calculated via a flash calculation (Walas, 1985), and the binary interaction parameters for the mixture of toluene and carbon dioxide in the temperature range of 25 to 200°C are 0.09 and 0 (Ng and Robinson, 1978; Dixon and Johnston, 1991).

The relative liquid expansion ($\Delta v/v_{\text{solvent}}$) is calculated from the total number of moles of both components in the liquid phase, $n_{\text{tot,liq}}$ (mol), normalized upon 1 mole of solvent and from the calculated molar volume of the expanded liquid phase v_{liq} ($\text{m}^3 \cdot \text{mol}^{-1}$):

$$n_{\text{tot,liq}} = \frac{1}{x_{\text{solvent}}} \tag{1}$$

where x_{solvent} is the mole fraction solvent in the liquid phase, and the total volume, $v_{\text{tot,liq}}$ (m^3):

$$v_{\text{tot,liq}} = n_{\text{tot,liq}} \cdot v_{\text{liq}} \tag{2}$$

The relative expansion of the liquid phase is

$$\frac{\Delta v}{v_{\text{solvent}}} = \frac{v_{\text{tot,liq}} - v_{\text{solvent}}}{v_{\text{solvent}}} \tag{3}$$

where v_{solvent} (m^3) is the volume of 1 mole of the pure solvent.

The equilibrium solubility of the solute in the liquid phase is related to the partial molar volume of the solvent. The partial molar volume of the expanded solvent $\bar{v}_{\text{solvent,mol}}$ ($\text{m}^3 \cdot \text{mol}^{-1}$) is calculated from the polynomial Peng and Robinson equation of state and is in a binary mixture given by

$$\bar{v}_{\text{solvent,mol}} = \frac{RT}{p}\left[Z^{\text{liq}} - x_1\left(\frac{\partial Z^{\text{liq}}}{\partial x_1}\right)\right] \tag{4}$$

where Z^{liq} is the calculated liquid-phase compressibility. The equilibrium solubility of the solute in the expanded liquid phase $w^*_{\text{eq}}(p,T)$ equals the equilibrium saturation solubility of the solute at atmospheric pressure $w^*_{\text{eq}}(p_0,T)$ times the ratio of the partial molar volumes of the solvent, only for positive values of the partial molar volume (Chang and Randolph, 1990b; Berends, 1994):

$$w^*_{\text{eq}}(p,T) = w^*_{\text{eq}}(p_0,T)\left[\frac{\bar{v}_{\text{solvent,mol}}(p,T)}{\bar{v}_{\text{solvent,mol}}(p_0,T)}\right] \tag{5}$$

where w^*_{eq} [kg solute (kg solvent)$^{-1}$] the equilibrium solubility of the solute is normalized per kilogram of solvent in the liquid phase.

Crystallization with a constant growth rate

The total surface area and crystal mass in a batch crystallizer are increasing in time. The Nývlt approach is adapted for the GAS process by calculating a pressure profile for the batch crystallizer that should lead to a constant supersaturation. Two ideal cases are presented, one starting with seeds, and one unseeded with a constant nucleation rate during the batch process time.

For batch crystallization with constant supersaturation the growth rate G (ms^{-1}) will be constant.

The Nývlt theory is derived with the following assumptions:

- The death function, due to agglomeration or breakage, is negligible.
- The birth function is restricted to the formation rate of nuclei at zero size and is constant for unseeded growth. In case of seeded growth no additional nucleation occurs.
- There is no slurry discharge during the batch crystallization cycle.
- The solution is ideally mixed.

The mass-balance for the GAS crystallizer equals

$$\frac{M_s dw^*}{dt} + \frac{dM_c}{dt} = 0 \tag{6}$$

where w^* [kg solute (kg solvent)$^{-1}$] is the total dissolved quantity of solute normalized per kilogram solvent, M_s (kg) is the amount of solvent and M_c (kg) is the total crystal mass in the crystallizer. The equilibrium solubility w^*_{eq} in the liquid phase is a function of the pressure in the crystallizer and is calculated with Eq. 5. The supersaturation σ of the solute in the liquid phase is presented by

$$\sigma = \frac{w^* - w^*_{\text{eq}}}{w^*_{\text{eq}}} \Rightarrow w^* = w^*_{\text{eq}}(\sigma + 1) \tag{7}$$

When σ is constant the mass balance is converted into

$$\frac{dw^*_{\text{eq}}}{dt} = -\frac{1}{(\sigma + 1)M_s}\frac{dM_c}{dt} \tag{8}$$

which gives the variation of the equilibrium solubility in time, and should therefore lead to the required pressure profile. Keeping the supersaturation constant actually requires that any raise in supersaturation by pressure increase must be just compensated by growth of the crystals, and thus that the allowable pressure increase rate is directly dictated by the actual crystal surface area.

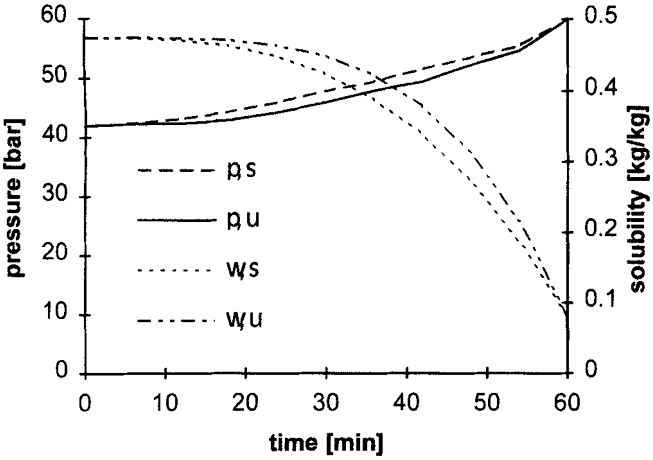

Figure 1. Required solubility and pressure time for phenanthrene to obtain constant supersaturation and growth rate, starting seeded (s) or unseeded (un) in the GAS crystallizer.

The desired equilibrium solubility as a function of the process time $w_{\mathrm{eq}}^{*}(t)$ becomes (Appendix A)

$$\frac{w_{\mathrm{eq}}^{*}(0) - w_{\mathrm{eq}}^{*}(t)}{w_{\mathrm{eq}}^{*}(0) - w_{\mathrm{eq}}^{*}(\tau)} = \left(\frac{t}{\tau}\right)^{\alpha} \tag{9}$$

where $\alpha = 3$ for seeded growth and $\alpha = 4$ for unseeded growth. With a given solubility at the start, $w_{\mathrm{eq}}^{*}(0)$, and at the end of the experiment, $w_{\mathrm{eq}}^{*}(\tau)$, and a selected growth time τ the required pressure profile as a function of time can be calculated.

The calculated equilibrium solubility and pressure curves for phenanthrene crystallizing from toluene with carbon dioxide as the antisolvent gas for a growth time of one hour is presented in Figure 1. The temperature is 25°C, the solubility in the crystallizer at atmospheric conditions is 0.47, and at the growth time τ assuming full expansion in the crystallizer at a final pressure of 60 bar the residual solubility in the crystallizer equals 0.08. Two curves are presented for the cases starting seeded or unseeded.

The curves start at 42 bar because a solution saturated at 1 bar does not become supersaturated until a pressure of 42 bar is reached. The measured phenanthrene solubility increases slightly up to approximately 42 bar after which the solubility drops rapidly with pressure up to 60 bar. The addition of seeds at a saturation pressure of 42 bar is not feasible. Seeds can, however, be created in situ by raising the pressure shortly above 42 bar. After the seeds are formed the pressure is lowered again to a pressure slightly above the saturation pressure of 42 bar. This produces seeds in the crystallizer at about the saturation pressure, although there is no real control of the number of seeds at the start of the experiment.

Experimental

Gas antisolvent equipment for crystallization

A drawing of the GAS equipment is presented in Figure 2 and in Berends (1994). Liquid carbon dioxide is cooled and pressurized with an air-driven pump (Williams, CRP1000W800B316TG). The pressurized liquid carbon dioxide enters a buffer vessel (Autoclave Engineers) where it is heated to a temperature between 25 and 35°C.

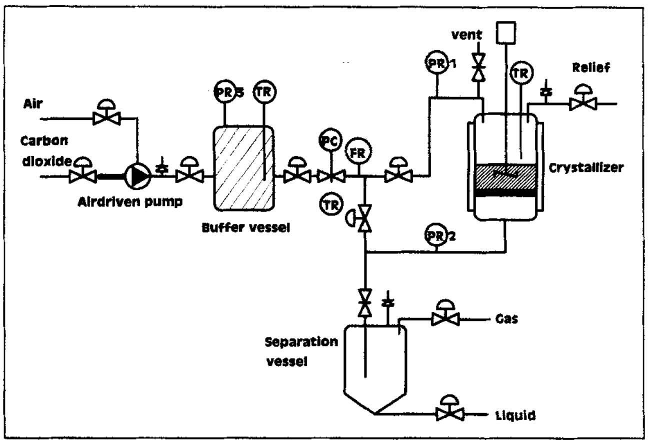

Figure 2. Drawing of the GAS equipment.

The 1-L crystallizer (Autoclave Engineers DD-100-SS-03AF-26DC) is for this purpose an adapted version of a standard 1-L autoclave equipped with a stirrer driven by an electrical motor with a magnetic coupling, two quartz sight glasses in the lid, and a sintered metal filter plate. The temperature in the crystallizer is controlled with a water jacket.

The carbon dioxide flow to the crystallizer is controlled with an air operated needle valve (Kämmer Ventile, 80037-I/P). To prevent its freezing, the needle valve is heated to the same temperature as the buffer vessel. The carbon dioxide can be fed to the crystallizer either through the bottom supply tube so that it bubbles through the liquid, or simultaneously through the top and bottom supply tubes so that no carbon dioxide bubbles through the liquid.

In the tubing to the crystallizer a coriolis-type mass flowmeter, FR (Micro Motion, DS 006 S 100), is placed to measure the total uptake of carbon dioxide during the different process steps.

A pressure transducer, PR2 (Wika, 891.23.510, accuracy 0.5%), measures the pressure drop over the filter plate during the filtration step. The filtered carbon dioxide toluene mixture is flashed to atmospheric conditions over a needle valve (Whitey, SS-31RS4) and separated in a liquid and gas phase in a separation vessel.

The pressure in the crystallizer during the filtration step is kept constant by admitting carbon dioxide to the top of the crystallizer. After the filtration step is completed, the solute is washed with pure carbon dioxide, the pressure in the crystallizer is let off, and the precipitated powder is collected.

Calibration of the toluene expansion

The GAS equipment was adapted to measure the expansion of toluene by replacing one of the metal bars that keeps the filter plate in position by a rod with five metal rings at different heights which can be seen through the quartz sight glasses. The heights of the metal rings were calibrated with water. The toluene expansion by carbon dioxide is measured at temperatures of 25, 40 and 65°C.

Experimental procedure for crystallization experiments

Chemicals. Phenanthrene (Janssen Chimica, 98 + %) was dissolved in toluene (Aldrich, 99% chemically pure). Solutions saturated at 25°C were used in quantities of 200 mL per experiment. The carbon dioxide was supplied by Air Products Inc., 99.95% pure.

Experimental Procedure. The filter plate is fitted in the crystallizer, the crystallizer is closed, and a pressure test is performed to assure that the system has no leaks. The experiment is started, the calculated pressure profile is completed, and only some temperature adjustments to the water bath have to be made to keep the crystallizer at the desired temperature; the rest of the controls run automatically. At the end of the experiment, the solution is filtered. After the pressure is reduced to atmospheric, the crystallizer is opened and the organic crystals are removed and analyzed.

Selected Process Parameters for the Experiments. The selected process parameters for the crystallization experiments are (i) the growth time, (ii) starting the growth period seeded or unseeded, (iii) the stirrer frequency (100 to 900 rpm), (iv) the temperature (25°C), (v) the initial saturation concentration, (vi) the carbon dioxide supply route (determines how the carbon dioxide is bubbling through the solution), and (vii) the final pressure, 60 bar.

Characterization of the Crystals. The phenanthrene crystals were analyzed by Scanning Electron Microscopy (SEM, JEOL JSM 5400) photographs to determine the number average particle size, particle-size distribution and particle morphology. The SEM is equipped with a cryostatic stage in the sputter coater and sample holder to prevent evaporation of the sample during the coating or scanning step.

The residual amount of toluene in the phenanthrene was determined by gas chromatography (Chrompack, CP 9001, silica column of 10 m, an internal diameter of 0.32 mm and a CP-SIL-5 coating with a thickness of 1.2 μm). XRD and LAUE photo's were used to determine the crystallinity.

The number average particle length d_{part} (m) as calculated from the SEM photographs is defined by

$$d_{\text{part}} = \frac{\sum_{i=1}^{N} d_{\text{part},i}}{N} \tag{10}$$

where N is the number of particles counted. In order to compare the width of two distributions the coefficient of variation C.V. is used, which is defined as

$$\text{C.V.} = \frac{\sigma}{d_{\text{part}}} = \frac{\sqrt{\dfrac{\sum_{i=1}^{N} (d_{\text{part},i} - d_{\text{part}})^2}{N}}}{d_{\text{part}}} \tag{11}$$

Results and Discussion

Relative liquid-phase expansion of toluene and carbon dioxide

The volumetric expansion of toluene and carbon dioxide vs. pressure at three different temperatures has been measured (Berends, 1994). The model predictions literature (Chang, 1990a,b) and the measured values are in good agreement, so the volumetric expansion in the autoclave follows the expected equilibrium.

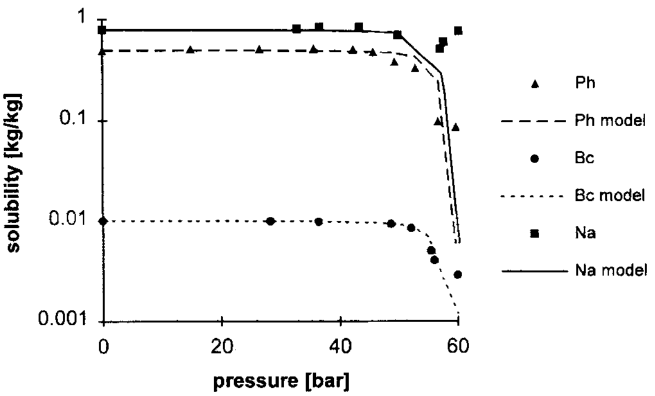

Figure 3. Solubility w^*_{eq} in the toluene carbon dioxide mixture for phenanthrene, naphthalene (Dixon and Johnston, 1991) and β-carotene (Chang, 1990a,b) as a function of the pressure at 25°C.

Comparison of calculated solubility curves of organics in toluene expanded by carbon dioxide with measured data from literature

The solubility of various solutes in a toluene carbon dioxide mixture as a function of pressure was obtained from literature. Dixon and Johnston (1991) measured the solubility of naphthalene and phenanthrene and Chang (1990a,b) the solubility of β-carotene in toluene and carbon dioxide at 25°C. The solubilities can also be calculated from the partial molar volume, as shown in Figure 3.

The results demonstrate that the solubility of these three component systems are predicted fairly well by binary data, considering that only toluene and carbon dioxide interaction factors are used for the calculations. Naphthalene deviates most from the calculated line, because it is easily soluble in compressed carbon dioxide at pressures above 50 bar. The solubility of β-carotene and phenanthrene is described more accurately because these compounds are less soluble in carbon dioxide.

The results reveal that the solubility in the liquid phase drops considerably at approximately the same pressure where the fast expansion of the liquid phase occurs. The solubility of naphthalene drops only slightly with a rising pressure, and after a minimum value is reached increases again to an even higher solubility than the equilibrium solubility at atmospheric pressure. This implies that it will be impossible to crystallize a reasonable amount of naphthalene from toluene with carbon dioxide as the antisolvent gas by the GAS process.

Pressure profile during an experiment

The pressure is the only process parameter that is not constant during the process. The pressure profile of a typical experiment can be divided into six periods as presented in Figure 4.

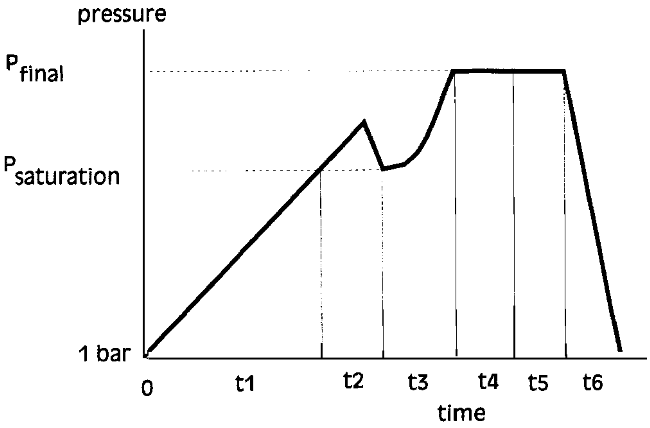

Figure 4. Pressure profile during a typical crystallization experiment.

For seeded operation the different process periods are

t1: Pressure Built-Up Period. In this period the pressure in the crystallizer is raised from atmospheric to the saturation pressure. For phenanthrene, this saturation pressure is approximately 42 bar. A period of 45 min was chosen arbitrarily.

t2: Pressure Pulse Period. In this period the pressure is raised to create nuclei, and when the liquid turns turbid the pressure is released again to a value near the saturation pressure and the growth period is started. This pressure pulse period lasts about 45 to 60 min.

t3: Growth Period. In this period the organic crystals are allowed to grow. The pressure profile should maintain a constant supersaturation. The growth time varied between 0.3 and 5 h.

t4: Holding Period. In this period the pressure is kept at its final value to enable the solution to expand and crystallize further. This holding time varied between 0 and 120 min.

t5: Filtration and Washing Period. In this period the solution is filtered over the filter plate by admitting carbon dioxide through the top of the crystallizer. After all toluene is removed, the crystals are washed by pure carbon dioxide. This period lasts from 20 to 45 min.

t6: Depressurizing Period. In this period the pressure is let off to atmospheric. This period should suffice to protect the O-rings against exploding and lasts from 15 to 30 min.

For unseeded operation the different process periods are the same as for seeded operation, except that the pressure pulse period t2 is skipped for unseeded operation.

Results of the phenanthrene experiments

During the experiments with phenanthrene, the theoretical pressure profile could be followed within 1 bar of the imposed curve and the tempertature could be maintained at 25 ± 2°C. The carbon dioxide was fed through the bottom of the autoclave so that it bubbles through the solution. From the filtered crystals, the number averaged particle size, the standard deviation of the distribution, the coefficient of variation, and the residual amount of toluene were measured. The average growth rate was calculated from the average particle size and the growth time. These data are presented in Table 1.

Number Average Particle Size and Particle-Size Distribution of Phenanthrene in Relation to the Process Conditions. The results presented in Table 1 show that the average particle size of the phenanthrene crystals can be influenced by a factor of 3, by varying the process conditions in the GAS process.

The results at a stirrer frequency of 300 rpm, exp. no. 65, 66 and 81, demonstrate that at a longer growth time, and thus at a lower supersaturation, larger crystals are produced, which is in accordance with theory.

A stirrer frequency of 900 rpm causes substantial attrition of the crystals, as is revealed by the SEM photographs of these crystals given in Figures 5 to 8. This explains why at this stirrer speed a longer growth time and no pressure pulse leads to smaller particle sizes, which decrease from 210 μm to a constant value of approximately 180 μm (see exp. no. 64, 61, 72, 73, 86 and 89). This attrition apparently counteracts the expected increase in size with longer growth times.

Table 1. Measured Number-Averaged Phenanthrene Particle Size, Standard Deviation of the Distribution, Coefficient of Variation and Residual Amount of Toluene and the Calculated Average Growth Rate of the Phenanthrene

Stirrer Freq. rpm	Growth Time h	Holding Time min	Pres. Pulse	d_{part} μm	C.V.	Growth Rate $\mu m \cdot s^{-1}$	Toluene ppm	Exp. No.
100	1.33	120	no	180	0.7	0.04	73	79
	5	30	no	200	0.5	0.01	50	80
300	0.5	0	no	240	0.3	0.14	105	65
	1	0	no	250	0.3	0.07	366	66
	5	30	no	300	0.4	0.02	37	81
300	0.33	50	yes	160	0.6	0.14	194	92
	5	30	yes	540	0.2	0.03	24	82
900	0.5	0	no	210	0.3	0.12	70	64
	1	0	no	200	0.3	0.06	82	61
	1.1	10	no	190	0.4	0.05	42	72
	1.1	40	no	180	0.3	0.05	59	73
	5	30	no	170	0.3	0.01	159	86
	5	30	no	190	0.2	0.01	227	89
900	0.33	15	yes	160	0.6	0.13	94	91
	5	30	yes	350	0.1	0.02	93	85
	5	30	yes	310	0.1	0.02	519	88

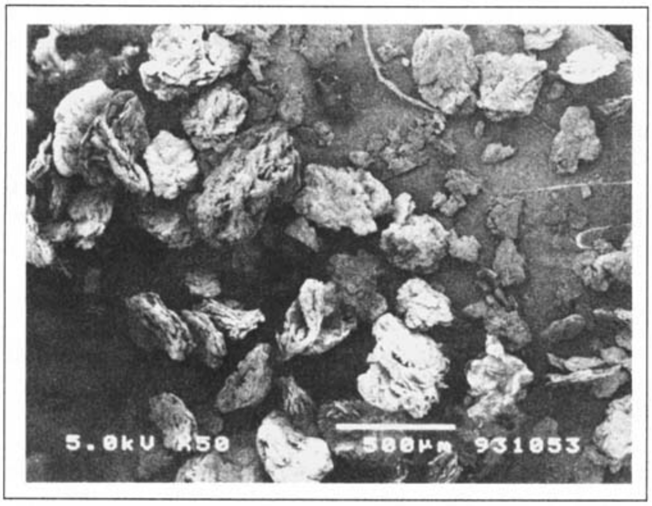

Figure 5. SEM photograph of phenanthrene with 5 h growth time, without a pressure pulse and 300 rpm, exp. no. 81.

The effect of the pressure pulse at the saturation pressure on the number averaged particle size and particle-size distribution is large:

- The averaged particle size is almost doubled from 300 to 540 μm (compare exp. no. 81 and 82 at 300 rpm or from 180 to 340 μm, compare exp. no. 86, 89, 85 and 88 at 900 rpm); and
- The particle-size distribution is significantly narrower, the coefficient of variation drops from 0.4 to 0.2 (compare exp. no. 81 and 82 at 300 rpm or from 0.3 to 0.1, compare exp. no. 86, 89, 85 and 88 at 900 rpm).

The presence of nuclei at the start of the pressure profile makes that growth of these nuclei the dominant factor process: this leads to a larger averaged particle size and a narrower particle-size distribution.

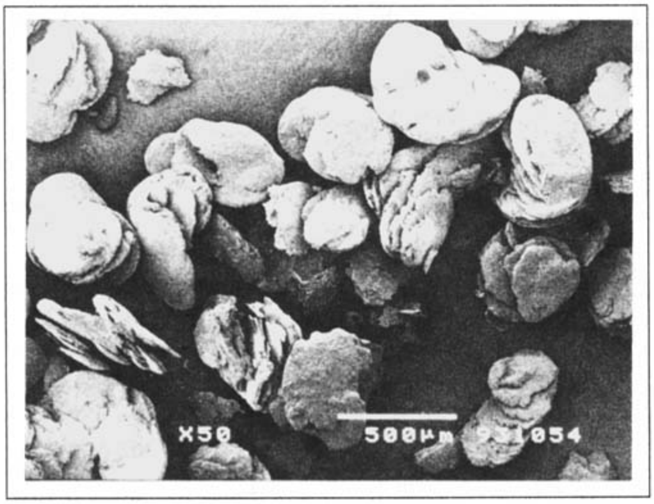

Figure 6. SEM photograph of phenanthrene with 5 h growth time, with a pressure pulse and 300 rpm, exp. no. 82.

Figure 7. SEM photograph of phenanthrene with 5 h growth time, without a pressure pulse and 900 rpm, exp. no. 86.

At 100 rpm the mass transfer of the carbon dioxide into the liquid phase proceeds too slowly, and the expansion profile does not follow the pressure profile at all. It takes up to two hours after the final pressure is reached before the liquid phase is fully expanded in the crystallizer.

The nonequilibrium between the gas and liquid phase causes a high supersaturation at the liquid gas interface and progressive primary nucleation can occur in this boundary layer. The result of this type of nucleation is that the crystals have a relatively larger standard deviation and thus a large coefficient of variation of 0.6 (exp. no. 79 and 80; see also the SEM photographs).

The SEM photographs of the experiments with a pressure pulse at 300 and 900 rpm (exp. no. 91 and 92) and with a growth time of only 20 min reveal the same kind of crystals with a large-size distribution and variation coefficient, as were

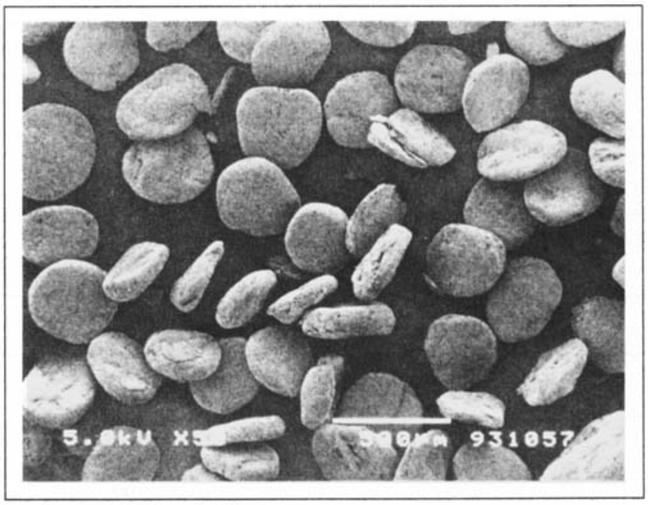

Figure 8. SEM photograph of phenanthrene with 5 h growth time, with a pressure pulse and 900 rpm, exp. no. 85.

Table 2. Residual Amount of Toluene in the Phenanthrene Crystals after Some Time, with or without Heating in an Oven at 50°C or After Extraction with Supercritical Carbon Dioxide at 60°C

Exp. No.	Toluene after Filtration ppm	Toluene after Treatment ppm	Treatment
61	82	34	Sample at room temp. for 56 d
64	70	49	Sample at room temp. for 37 d
65	105	52	Sample at room temp. for 36 d
73	59	21	Sample in an oven at 50°C for 26.5 h
86	159	12	Sample extracted with supercritical CO_2 at 175 bar and 60°C for 5 h

formed for the experiments at 100 rpm. A growth time of 20 min is apparently too short to get a homogeneous liquid phase without large supersaturation gradients at the liquid-gas interface that result in progressive nucleation.

Residual Amount of Toluene in the Phenanthrene Crystals. The residual amount of toluene in the precipitated phenanthrene varied between 24 and 519 ppm, as presented in Table 1. The results show no reproducible influence of the process parameters, that is, the growth time, holding time, stirrer frequency or pressure pulse, on the residual amount of toluene in the crystallized phenanthrene.

To determine whether the toluene only adheres to the crystals or is enclosed in the crystals as liquid inclusions, the residual amount of toluene in the phenanthrene crystals was measured again after some time, with or without heating in an oven at 50°C or after extraction with supercritical carbon dioxide at 60°C. These results are presented in Table 2.

The residual amount of toluene in the phenanthrene crystals drops significantly in 36 to 56 days even when the crystals are kept at room temperature. Heating of the crystals in an oven at 50°C for 26.5 h or extraction with supercritical carbon dioxide reduced the residual amount of toluene down to 12 ppm.

If the toluene would be enclosed in the phenanthrene crystals, the removal of toluene could only proceed by solid state diffusion, which is extremely slow or by diffusion via grain boundaries and dislocations, which is also expected to be a slow process. The toluene is thus likely not to be enclosed in the crystals but is attached to the surface of the crystals that form the agglomerates.

Characteristics of the Phenanthrene Crystals. The cryo SEM photographs of the phenanthrene particles produced in experiments with a 5-h growth time and 300 rpm (Figures 5 and 6) show that pressure pulse seeding makes larger particles. The particle structure in case of pressure pulse seeding also seems to be more compact with better packed platelets with parallel {001} faces. LAUE photographs of single particles show that these consist of an agglomerate of stacked platelets. The particles produced with a pressure pulse are composed of larger monocrystalline platelets than without the pressure pulse.

The cryo SEM photographs of the phenanthrene particles produced in experiments with a 5-h growth time and 900 rpm (Figures 7 and 8) show that the particles are more rounded, more uniform in size and smaller than the particles made with a stirrer frequency of 300 rpm. At 900 rpm, attrition is a predominant factor which can be seen especially for the particles grown with pressure pulse seeding. LAUE photographs of single particles show that these again consist of an agglomerate of crystals. These photographs also show that the sizes of the single crystalline domains are smaller than for the 300 rpm experiment, owing to the larger attrition at this stirrer frequency. The particles produced with a pressure pulse are composed of larger monocrystalline platelets than without the pressure pulse.

The phenanthrene particles grown in 1.33 h with a stirrer frequency of 100 rpm have a particle-size distribution that is very wide, and singular platelets can be seen which are probably grown at the gas-liquid interface at a large supersaturation. Geertman (1994) observed similar platelets during the growth of biphenyl crystals from toluene at the gas-liquid interface and Gallagher (1992) also observed the formation of platelets of RDX at the gas-liquid interface. The bulk fluid phase is not or only slightly supersaturated so the particles show here no further agglomeration or growth.

At 100 rpm and a longer growth time of 5 h, the particles do not show so many lose platelets: they are more agglomerated. This may be explained by the slower buildup of supersaturation which causes a smaller gradient across the boundary layer.

The phenanthrene particles of experiments 92 and 91 with a 20 min growth time and a pressure pulse have the same kind of platelet structure as the 100 rpm experiments. The 300 rpm experiment show more loose "platelets" than for the 900 rpm experiment. The mass transfer is better for the 900 rpm than for the 300 rpm experiment, so in the first case a smaller concentration gradient exists at the interface and growth and agglomeration occur mainly in the bulk fluid phase leading to more agglomerated particles. The growth time of 20 min is apparently insufficient to avoid mass-transfer problems at the gas-liquid interface.

It can be concluded that agglomeration is an important factor in the GAS process. The stirrer frequency determines the degree of attrition that occurs in the GAS process, 100 rpm none, 900 rpm significantly, as well as the mass-transfer rate of the anti-solvent gas into the liquid phase.

Conclusions

The expansion of the liquid phase by dissolving compressed carbon dioxide in toluene increases slowly with increasing pressure until at a certain pressure the expansion increases very steeply, almost exponentially. At a higher liquid-phase temperature, a higher pressure is needed to obtain the same liquid-phase expansion.

The measured liquid-phase expansion in the GAS crystallizer equals the liquid-phase expansion calculated from the Peng and Robinson equation of state.

The solubility of the solute in the expanded liquid is predicted well by the partial molar volume of the toluene, as long as the solute does not dissolve in the compressed carbon dioxide with the toluene as an entrainer. The solubility first increases slightly with increasing pressure, but when the fast expansion occurs the solubility starts to drop equally fast. Components that dissolve in the high-pressure carbon dioxide are not suitable for crystallization with the GAS process. From literature solubility data, it can be calculated that crystallizing naphthalene from toluene with carbon dioxide as the anti-solvent gas is not feasible.

The averaged particle size of phenanthrene crystallizing from toluene with carbon dioxide added as the anti-solvent gas by a pressure profile scheme could be varied by a factor of 3: from 160 to 540 μm. At 300 rpm the particle size increases at a prolonged growth time and thus at a lower supersaturation, as was expected. At 900 rpm without a pressure pulse, however, the particle size reduces at an increased growth time due to attrition of the crystals. Creation of the seeds at the saturation pressure doubles the particle size and makes the particle-size distribution and coefficient of variation significantly smaller.

The 100 rpm experiments and the experiments with a 20-min growth time and a pressure pulse produce small particles of a 160-μm size with a very wide distribution. This comes from a too slow mass-transfer rate of the compressed carbon dioxide gas into the liquid phase which leads to progressive nucleation at the gas-liquid interface.

The residual amount of toluene in the phenanthrene crystals is significantly better than for normally grown phenanthrene and can be reduced even more by extraction with supercritical carbon dioxide or by heating of the particles in an oven.

The SEM photographs show that the particle structure in case of pressure pulse seeding seems to be more compact with better packed platelets with parallel {001} faces. LAUE photographs of single particles show that these particles consist of an agglomerate of stacked platelets. The particles produced with a pressure pulse are composed of larger monocrystalline platelets than without the pressure pulse. Agglomeration is thus an important factor in the GAS process.

The stirrer frequency determines the degree of attrition that occurs in the GAS process, 100 rpm none, 900 rpm significantly, as well as the mass-transfer rate of the anti-solvent gas into the liquid phase.

Acknowledgments

The authors would like to thank T. J. G. Collot d' Escury and A. C. H. van den Engel for their contributions to this study.

Notation

A = total crystal surface area (m^2)
C = nucleation rate constant (#s^{-1})
C.V. = coefficient of variation
G = growth rate (ms^{-1})
k_a = surface area shape factor
k_v = volume shape factor
l_s = length of the uniform seeds (m)
L = total crystal length (m)
M_s = mass of solvent (kg)
n = number of moles
N = total number of crystals
N = number of crystals counted
p = pressure (Pa)
R = ideal gas constant (J·mol^{-1}·K^{-1})
t = time (s)
T = temperature (K)
v = molar volume (m^3·mol^{-1})
$\bar{v}_{\mathrm{solvent,mol}}$ = partial molar volume (m^3·mol^{-1})
w^*_{eq} = solubility [kg solute (kg solvent)$^{-1}$]
x = mole fraction in 1 phase
Z = compressibility

Greek letters

α = correction factor
ρ_c = crystal density (kg·m^{-3})
σ = supersaturation
σ = standard deviation (m)
τ = growth time (s)

Superscripts

liq = liquid phase
vap = vapor phase

Subscripts

c = critical
c = crystal
eq = equilibrium
i = component i
j = component j
0 = reference state

Literature Cited

Berends, E. M., "Supercritical Crystallization: The RESS-Process and the GAS-Process," PhD Thesis, Delft Univ. of Technology, Delft (1994).

Chang, C. J., "Recrystallization of Organic Compounds from Supercritical Fluids and High-Pressure Gas-Expanded Liquid Solvents," PhD Thesis, Univ. of Arizona, Tucson, AZ (1990a).

Chang, C. J., and A. D. Randolph, "Solvent Expansion and Solute Solubility Predictions in Gas-Expanded Liquids," *AIChE J.*, **36**(6), 939 (1990b).

Dixon, D. J., and K. P. Johnston, "Molecular Thermodynamics of Solubilities in Gas Antisolvent Crystallization," *AIChE J.*, **37**(10), 1441 (1991).

Dixon, D. J., K. P. Johnston, and R. A. Bodmeier, "Polymeric Materials formed by Precipitation with a Compressed Fluid Antisolvent," *AIChE J.*, **39**(1), 127 (1993).

Gallagher, P. M., M. P. Coffey, V. J. Krukonis, and N. Klasutis, "Gas Anti-Solvent Recrystallization: New Process to Recrystallize Compounds Insoluble in Supercritical Fluids," In: *Supercritical Fluid Science and Technology*, K. P. Johnston and J. M. L. Penninger, eds., ACS Symp. Ser., **406** American Chemical Society, Washington, D.C., p. 334 (1989).

Gallagher, P. M., M. P. Coffey, V. J. Krukonis, and W. W. Hillstrom, "Gas Anti-Solvent Recrystallization of RDX: Formation of Ultra-Fine Particles of a Difficult-to-Comminute Explosive," *J. of Supercritical Fluids*, **5**(2), 130 (1992).

Geertman, R. M., Private communication (1994).

Ng, H. J., and D. B. Robinson, "Equilibrium Phase Properties of the Toluene-Carbon Dioxide System," *J. Chem. Eng. Data*, **24**(4), 325 (1978).

Nývlt, J., "Batch Crystallizer Design," *Advances in Industrial Crystallization*, J. Garside, R. J. Davey, and A. G. Jones, eds., Butterworth-Heineman Ltd., Oxford, pp. 197–212 (1991).

Peng, D.-Y., and D. B. Robinson, "A New Two Constant Equation of State," *Ind. Eng. Chem. Fundam.*, **15**(1), 59 (1976).

Walas, S. M., *Phase Equilibria in Chemical Engineering*, Butterworth Publishers, Boston (1985).

Appendix: Derivation of the Nývlt Theory for a Constant Growth Rate

Case 1: seeds added and no nucleation during the experiment

The next equations can be derived for the first four moments of the crystal-size distribution in the crystallizer starting with N_0 uniform seeds of length l_s:

$$\frac{dN}{dt} = 0 \qquad \text{with} \quad N(0) = N_0;\ N(t) = N_0 \qquad \text{(A1)}$$

$$\frac{dL}{dt} = NG \qquad \text{with} \quad L(0) = N_0 l_s \tag{A2}$$

$$\frac{dA}{dt} = 2k_a LG \qquad \text{with} \quad A(0) = N_0 k_a l_s^2 \tag{A3}$$

$$\frac{dM_c}{dt} = \frac{3\rho_c k_v AG}{k_a} \qquad \text{with} \quad M_c(0) = N_0 k_v \rho_c l_s^3 \tag{A4}$$

where $N = N_0$ is the total number of crystals (= constant in time; no nucleation), L (m) is the total crystal length, l_s (m) is the length of the uniform seeds, A (m^2) is the total crystal surface area in the crystallizer, k_a and k_v are the surface area and volume shape factor and ρ_c (kg · m^{-3}) is the crystal density.

The required variation of the total crystal mass in the crystallizer as a function of time is

$$\frac{d^3M_c}{dt^3} = \frac{3\rho_c k_v G}{k_a}\frac{d^2A}{dt^2} = 6\rho_c k_v G^2 \frac{dL}{dt} = 6\rho_c k_v G^3 N \tag{A5}$$

This third-order differential equation has no time dependent parameters and can be integrated with the boundary conditions at $t = 0$ which are

$$M_c(0) = N_0 k_v \rho_c l_s^3 \tag{A6}$$

$$\frac{dM_c(0)}{dt} = 3\rho_c k_v N_0 l_s^2 G \tag{A7}$$

$$\frac{d^2M_c(0)}{dt^2} = 6\rho_c k_v N_0 l_s G^2 \tag{A8}$$

This leads to

$$M_c(t) = \int\int\int 6\rho_c k_v N G^3 dt dt dt$$

$$= 3\rho_c k_v N_0 G^3 \frac{1}{3} t^3 + 3\rho_c k_v N_0 l_s G^2 t^2 + 3\rho_c k_v N_0 l_s^2 G t + M_c(0)$$

$$= 3\rho_c k_v N_0 l_s^3 \left\{ \frac{1}{3}\left(\frac{Gt}{l_s}\right)^3 + \left(\frac{Gt}{l_s}\right)^3 + \left(\frac{Gt}{l_s}\right) \right\} + M_c(0) \tag{A9}$$

If $Gt/l_s \gg 1$, the total crystal mass as a function of the process time t [s] with a growth time τ [s] can be simplified to

$$\frac{M_c(t) - M_c(0)}{M_c(\tau) - M_c(0)} = \left(\frac{t}{\tau}\right)^3 \tag{A10}$$

With Eq. 9, the desired equilibrium solubility as a function of the process time $w^*_{\text{eq}}(t)$ [kg solute (kg solvent)$^{-1}$] becomes

$$\frac{w^*_{\text{eq}}(0) - w^*_{\text{eq}}(t)}{w^*_{\text{eq}}(0) - w^*_{\text{eq}}(\tau)} = \left(\frac{t}{\tau}\right)^3 \tag{A11}$$

With a given solubility at the start $w^*_{\text{eq}}(0)$ and at the end of the experiment $w^*_{\text{eq}}(\tau)$ with a selected growth time τ, the required pressure profile as a function of time can be calculated.

Case 2: no seeds added and a constant nucleation rate

The next equations can be derived for the first four moments of the crystal-size distribution in the crystallizer:

$$\frac{dN}{dt} = \text{constant} = C \qquad \text{with} \quad N(0) = 0 \tag{A12}$$

$$\frac{dL}{dt} = NG \qquad \text{with} \quad L(0) = 0 \tag{A13}$$

$$\frac{dA}{dt} = 2k_a LG \qquad \text{with} \quad A(0) = 0 \tag{A14}$$

$$\frac{dM_c}{dt} = \frac{3\rho_c k_v AG}{k_a} \qquad \text{with} \quad M_c(0) = 0 \tag{A15}$$

The required variation of the total crystal mass in the crystallizer as a function of time is

$$\frac{d^4M_c}{dt^4} = \frac{3\rho_c k_v G}{k_a}\frac{d^3A}{dt^3} = 6\rho_c k_v G^2 \frac{d^2L}{dt^2} = 6\rho_c k_v G^3 \frac{dN}{dt} = 6\rho_c k_v G^3 C \tag{A16}$$

This fourth-order differential equation has no longer time dependent parameters and can be integrated with the boundary conditions at $t = 0$ which are

$$\frac{d^3M_c(0)}{dt^3} = \frac{d^2M_c(0)}{dt^2} = \frac{dM_c(0)}{dt} = M_c(0) = 0 \tag{A17}$$

This leads to

$$M_c(t) = \int\int\int\int 6\rho_c k_v C G^3 dt dt dt$$

$$= \frac{\rho_c k_v C G^3}{4} t^4 + M_c(0) \tag{A18}$$

The total crystal mass as a function of the process time t [s] with a growth time τ [s] can be simplified to

$$\frac{M_c(t) - M_c(0)}{M_c(\tau) - M_c(0)} = \left(\frac{t}{\tau}\right)^4 \tag{A19}$$

With Eq. 9, the desired equilibrium solubility as a function of the process time $w^*_{\text{eq}}(t)$ [kg solute (kg solvent)$^{-1}$], becomes:

$$\frac{w^*_{\text{eq}}(0) - w^*_{\text{eq}}(t)}{w^*_{\text{eq}}(0) - w^*_{\text{eq}}(\tau)} = \left(\frac{t}{\tau}\right)^4 \tag{A20}$$

With a given solubility at the start $w^*_{\text{eq}}(0)$ and at the end of the experiment $w^*_{\text{eq}}(\tau)$ with a selected growth time τ, the required pressure profile as a function of time can be calculated.

Manuscript received Oct. 11, 1994, and revision received Mar. 22, 1995.